Analysis on Missile-borne Bistatic Forward-looking SAR Imaging Perfomance

Qi Chen[1,2,a], Xiangping Li[1], Mingbo Zhu[1] and Xiaohai Zou[1,2]

[1]*Naval Aeronautical and Astronautical University, Department of Electronic and Information Engineering, 264001 Yantai, China*
[2]*CEMEE State Key Laboratory, 471003 Luoyang, China*

Abstract. Synthetic aperture radar (SAR) has been gradually applied to missile guidance for its advantages of all-weather, all-time and long-distance capabilities. Nevertheless, missile-borne SAR can not image on the area in front of the missile track restricted by SAR working characteristics. Missile-borne forward-looking SAR will be realized through separated transmitter and receiver. Iso-range contours, iso-Doppler contours, ground resolution and azimuth resolution are used to analyze the performance of missile-borne bistatic forward-looking SAR, as to provide the theoretical basis for its application.

1 Introduction

In modern war, missile-based precision guided weapons have been the key restrictor that determines the process and the result of the war, making lots of countries compete for the development on them[1]. Infrared guidance, television guidance and radar guidance are the traditional ways for missile guidance, among which radar guidance has a good application prospect for its all-weather and all-time capabilities[2-4]. Missile-borne SAR guidance can provide two-dimensional images with high resolution, which has a number of advantages over one-dimensional imaging guidance. However, SAR can not image on the area in front of the platform track limited by the inherent working characteristics. Thus missile-borne SAR can only be used in matching guidance through side-looking or squint-looking imaging rather than homing guidance, restricting its application scenarios. The emergence of bistatic SAR offers a new way to solve this problem[5-8]. Bistatic SAR realizes forward-looking through separated transmitter and receiver, making up the inherent disadvantages of monostatic SAR. Iso-range contours, Iso-Doppler contours, ground resolution and azimuth resolution are used in this paper to research the feasibility of missile-borne bistatic forward-looking SAR.

2 Geometric model

The geometric model of missile-borne bistatic forward-looking SAR is shown in Figure 1.

[a] Corresponding author : chenqiyt@163.com

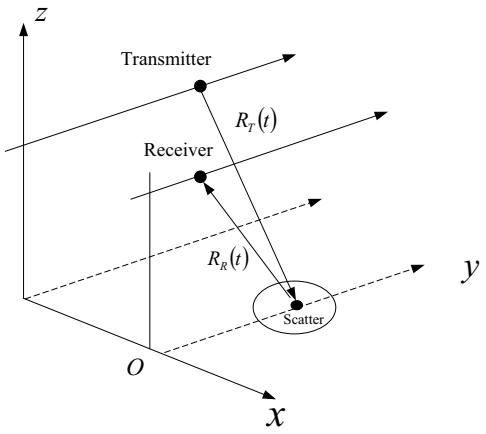

Figure 1. Geometric model of bistatic forward-looking SAR

The transmitter and receiver point together to the front area of receiver in the figure. The signals are transmitted to the target area in a certain PRT, then received and recorded by the receiver. $R_T(t)$ is the squint distance between the transmitter and the scatter, $R_R(t)$ is the squint distance between the receiver and the scatter.

3 Iso-range contours and iso-Doppler contours

Different scatters are distinguished through their distance to bistatic system in range direction. The range distance determines the time delay of the echo signal. The expression of range distance is

$$R(t) = R_T(t) + R_R(t) \tag{1}$$

Iso-range contours are composed of scatters with the same range distances, which are always in the form of ellipse.

The Doppler frequency of bistatic SAR is

$$f = -\frac{1}{\lambda}\left(V_T I_T(t) + V_R I_R(t)\right) \tag{2}$$

Where V_T and V_R are the velocities of the transmitter and receiver, respectively. $I_T(t)$ and $I_R(t)$ are the unit vector from the transmitter and receiver antenna phase centers to the scatter, respectively. Iso-Doppler contours are composed of scatters with the same Doppler frequency.

SAR system can obtain two-dimensional image of the area where the iso-range contours and iso-Doppler contours make rectangle or approximate rectangular partition.

When $V_T = V_R$, $R_T(t) = R_R(t)$, (3) and (4) refer to the calculation equation of monostatic SAR. The iso-range contours and iso-Doppler contours of an ordinary monostatic SAR system are shown in Figure 2. The arrow in the figure symbolizes the location and move direction of the SAR system. As is shown in the picture, the areas in side-looking and squint-looking direction have orthorhombic iso-range contours and iso-Doppler contours, indicating the nice imaging performance in these areas. Meanwhile, the The approximatively parallel iso-range contours and iso-Doppler contours in forward-looking direction account for the poor imaging performance in that areas.

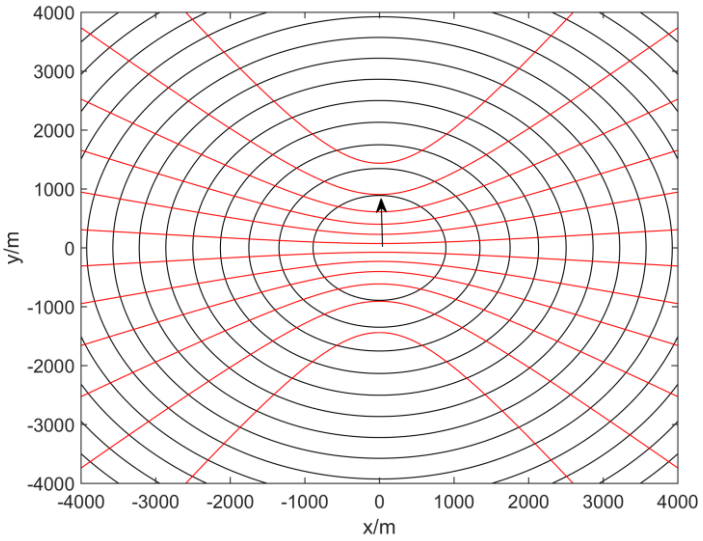

Figure 2. Monostatic SAR iso-range contours (circles) and iso-Doppler contours (lines)

4 Ground resolution and azimuth resolution

Derivated from the gradient method, the expression of bistatic SAR ground resolution is

$$\rho_{rG} = \frac{c}{B\sqrt{2+2\cos\beta-\left(\cos\phi_T+\cos\phi_R\right)^2}} \tag{3}$$

Where c is light velocity, B is signal bandwidth, β is bistatic angle, ϕ_T , ϕ_R are the incidence angles of transmitter and receiver, respectively.

The expression of bistatic SAR azimuth resolution is

$$\rho_a = \frac{D_R}{\sin^2\theta_R + K_V^2 / K_R \sin^2\theta_T} \tag{4}$$

Where K_V is the transmitter to receiver velocity ratio, K_R is the transmitter to receiver range distance ratio at center moment of synthetic aperture, D_R is the azimuth size of receiver antenna, θ_T and θ_R are coangles of transmitter and receiver squint angle, respectively.

5 Simulation and analysis

Assume a bistatic SAR system in which the missile-borne transmitter is working on side-looking mode, the missile-borne receiver is working in forward-looking mode. Parameter Settings are shown in Table 1, iso-range contours and iso-Doppler contours are shown in Figure 3, distribution curves of ground resolution are shown in Figure 4 and distribution curves of azimuth resolution are shown in Figure 5.

Table 1. Simulation parameters

Parameters	Values
Wavelength	0.03 m
Pulse bandwidth	200 MHz
Pulse width	2 μs
Azimuth size of transmitter and receiver antennas	1 m
PRF	2500 Hz
Transmitter velocity	(0,500,0) m/s
Receiver velocity	(0,500,0) m/s
Initial position of transmitter	(-6000,0,1000) m
Initial position of receiver	(0,-6000,1000) m

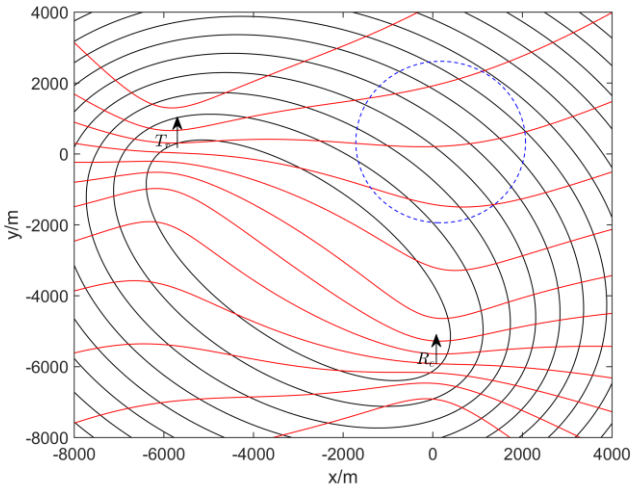

Figure 3. Bistatic SAR Iso-range contours (circles) and iso-Doppler contours (lines)

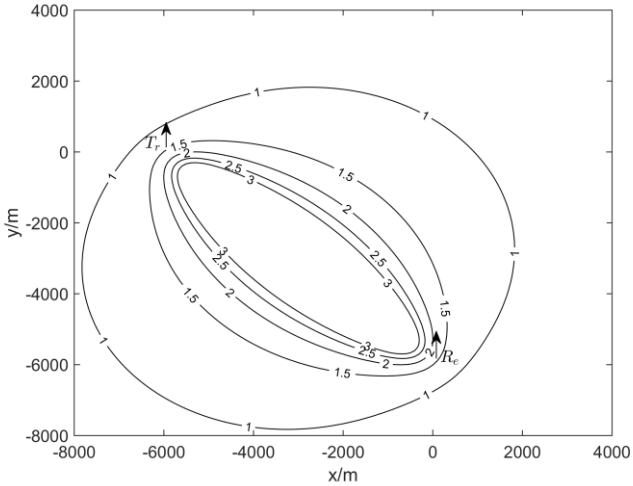

Figure 4. Ground resolution distribution curves

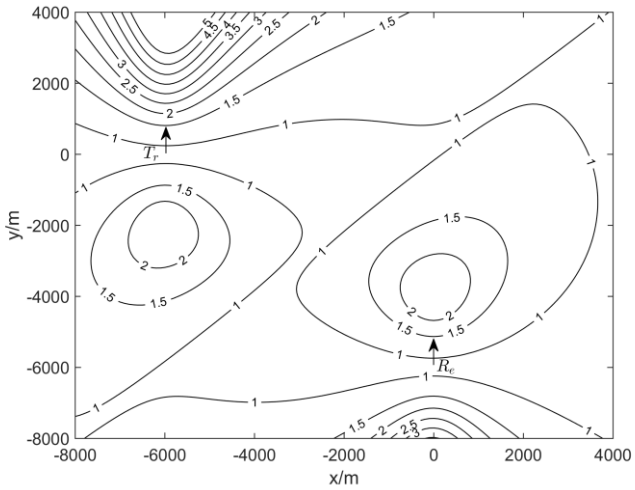

Figure 5. Azimuth resolution distribution curves

T_r and R_e are transmitter and receiver, respectively. The dashed part in Figure 3 is the imaging area. It is observed that the iso-range contours and iso-Doppler contours form rectangular segmentations in the imaging area, which indicates the forward-looking ability of the receiver. Therefore, the bistatic SAR system has high ground and azimuth solutions in the imaging area, as is shown in Figure 4 and Figure 5.

Echo simulation and imaging process are conducted for the point target at (0,0,0). Point target simulation result is shown in Figure 6. The result tells the well focus in range and azimuth directions, which validates the correctness of the above conclusion.

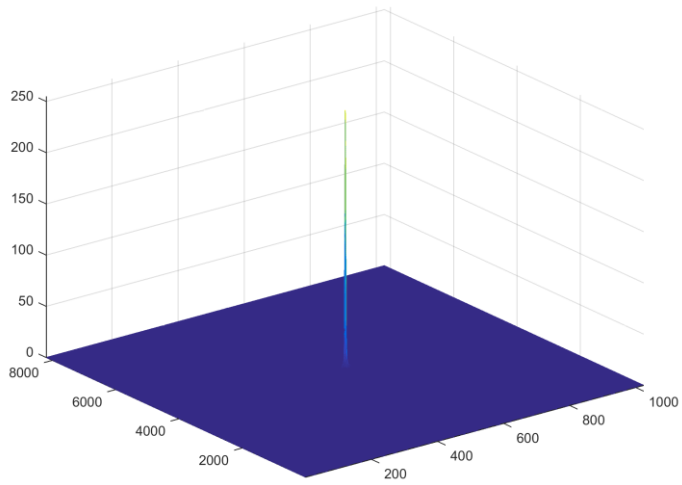

Figure 6. Simulation result of point target

6 Conclusions

To verify the imaging performance of missile-borne bistatic forward-looking SAR, the iso-range contours and iso-Doppler contours of the system in which the transmitter is side-looking and the receiver is forward-looking are depicted. Then the ground and azimuth resolution calculation and point target simulation reveals the imaging ability of missile-borne bistatic forward-looking SAR. The results show that bistatic forward-looking SAR can be applied to missile platform. In practice, the transmitter can be placed on an UAV, a reconnaissance aircraft or a missile to illuminate along with the forward-looking missile-borne receiver to image the target area and realize forward-looking SAR guidance, which has a high application value.

Acknowledgments

This work is sponsored by open research foundation of State Key Laboratory (CEMEE2016K0201B).

References

1. H Wei, G Min. AMJ, **8**, 56 (2016).
2. ZH Zhaorong, G He, ZH Xi, L Tao, K Yuhang. AMJ, **3**, 23 (2016).
3. L Qi, Q Luyan. IT, **1**, 146 (2016).
4. ZH Gang, ZH Mingbo, ZH Zhenbo, L Xiangping. AMJ, **9**, 67 (2011).
5. Y Jianyu, H Yulin, Y Haiguang, W Junjie, L Wenchao, L Zhongyu, Y Xiaobo. IGARSS, 4202 (2013).
6. W Ingo, E Thomas, K Jens, R. B. Andreas, H. G. E. Joachim. IGARSS, 216 (2010).
7. E Thomas, W Ingo, K Jens, R. B. Andreas, H. G. E. Joachim. GRSL, **8**, 765 (2011).
8. W Ingo, R. B. Andreas, K Jens. IGARSS, 327 (2012).